ELSEVIER

Inorganic Chemistry Communications 5 (2002) 181–186

INORGANIC CHEMISTRY COMMUNICATIONS

www.elsevier.com/locate/inoche

The divalent cation-induced DNA condensation studied by atomic force microscopy and spectra analysis

Xue-Guang Sun [a], En-Hua Cao [a,*], Xiao-yan Zhang [a], Dage Liu [b], Chunli Bai [b]

[a] *Institute of Biophysics, The Chinese Academy of Sciences, 15 Datun Road, Chaoyang District, Beijing 100101, China*
[b] *Institute of Chemistry, The Chinese Academy of Sciences, Beijing 100080, China*

Received 31 July 2001; accepted 5 December 2001

Abstract

Three types of DNA condensates in the presence of divalent metal ion (Mg, Mn and Cu) and EB simultaneously have been observed by atomic force microscopy (AFM). In the presence of Mg (II) and EB, DNA molecular exhibits three or four maggot-like branch crossing structures at the same point, which were constructed by some bead-like particles in each branch. However, in the presence of Cu (II) or Mn (II)–EB, DNA molecular forms a network or a semicircular structure, respectively. Their average height was 0.95 ± 0.5 nm (Cu (II)–DNA–EB), 17 ± 5 nm (Mg (II)–DNA–EB) and 12 ± 3 nm (Mn (II)–DNA–EB), respectively. However, DNA molecular or DNA–EB complex still remained a line double-stranded structure. The fluorescence, melting point and CD spectra indicate that the different morphologies induced by divalent metal ion (Mg (II), and Mn (II) and Cu (II)) are related to its binding position in molecular DNA.

Keywords: Atomic force microscopy; DNA condensation; Divalent metal cation; DNA; Circular dichroism

Abbreviations: EB (Ethidium bromide); CD (Circular Dichroism); AFM (Atomic force microscopy)

1. Introduction

Divalent metal ions are widely presented in vivo, and known to be essential for living organisms to maintain regular activities [1]. Usually, transition metals have a strong base-affinity. They can chelate or coordinate directly to the nucleophilic atoms of bases; thus perturb the hydrogen bonding between base pairs, resulting in a destabilization of DNA. Conversely, alkaline earth cations with greater binding specificity for the phosphates can neutralize the negative charge of sugar–phosphate backbone and enhance the base stacking [2]. The two bindings are both capable of altering the geometry of a nucleotide. Some investigations demonstrated that divalent metal ions not only can induce DNA condensation [3] or aggregation [4], but also can alter its secondary or tertiary structure [5–7]. This makes metal ions serve as a potential modulator of DNA function. Thus, studies on DNA condensation have potential biological significance and have increasingly received attention [8].

On other hand, interactions of DNA with ligand have been studied extensively for several decades due to their biological application, as an anticancer drug, probes of nucleic acid damage and structure [9] and as sequence-specific binding and cleavage agents [10]. However, the morphology characteristic of DNA complex structure in the presence of ligand and cation is still unclear and cannot be observed directly.

In this present study, we choose a fluorescence probe, ethidium bromide, as the ligand of DNA to study the formation and structure characteristics of DNA complex in the presence of three divalent cations and EB, using an atomic force microscopy (AFM). Three types of DNA condensates with different morphologies have been observed directly. Results of fluorescence, CD spectrum and melting point indicate that the different morphologies induced by Cu (II) Mg (II) and Mn (II) were related to its binding position in molecular DNA.

* Corresponding author. Tel.: +86-10-64888567; fax: +86-10-64877837.
E-mail address: caoeh@sun5.ibp.ac.cn (E.-H. Cao).

1387-7003/02/$ - see front matter
PII: S1387-7003(02)00320-9

2. Materials and methods

2.1. Chemicals and nucleic acid

Chloride salts of magnesium, manganese and copper (analytical grade) were obtained from Aldrich (Milwaukee, WI) and dissolved, respectively, in the purified water, forming a 1 M solution. Calf thymus DNA (Sigma Type I) was dissolved at 1 mg/ml in Milli-Q water and stirred overnight to obtain a uniform solution. Ethidium bromide was purchased from Sigma. Stock solution was made up in water and protected from light. Concentration was determined by direct weighing.

2.2. Fluorescence measurement

All fluorescent measurements were made on a Hitachi M850 model spectrofluorometer. Fluorescence emission spectra were recorded with excitation at 510 nm or emission at 620 nm, respectively.

Energy transfer from DNA to the bound ethidium was measured from the excitation spectra and corresponding absorption spectra of the DNA/ethidium complex in the wavelength range from 220 to 310 nm. In order to decrease the inner filter effect, a correction factor (exp[a/2], the absorption) is applied. $Q = q_b/q_t$ (q_b or q_t is the relative quantum yield of bound or free ethidium, respectively) was calculated for each wavelength using the following equation: $Q_\lambda/Q_{310} = [I_bE_f/I_fE_b]_\lambda/[I_bE_f/I_fE_b]_{310}$, where I is the fluorescence intensity of ethidium and E, the corresponding ethidium molar extinction coefficient. Then, the ratio Q_λ/Q_{310} was plotted against wavelength [11].

2.3. Analysis of melting profiles

The UV melting experiments were carried out on a Hitachi U-3200 spectrophotometer. Sample temperature was controlled by an external circulating water bath, at a heating rate of 0.25 °C/min, monitoring the absorption change at 260 nm.

The experimental melting profile is converted to a plot of α (the helix–coil transition fraction) vs temperature. It is normalized by taking the ratio at each temperature of the height between the experiment curve $A_{260}(T)$ and the lower baseline $A_D(T)$ and the height between the lower $[A_D(T)]$ and upper $[A_U(T)]$ baseline, i.e. $\alpha(T) = [A_{260}(T) - A_D(T)]/[A_U(T) - A_D(T)]$.

2.4. Circular dichroism spectrum

CD spectra were recorded on a Jasco 700 spectropolarimeter, using a cell of 1 mm path length. Sample temperature was controlled by an external circulating water bath. All CD spectra were averaged over eight acquisitions with a scan rate of 50 nm/min and a time constant of 1 s. All CD data were baseline-corrected for signals due to the cell and buffer.

2.5. Atomic force microscopy observation

A 2 μl drop of the DNA–EB solutions (the concentration of DNA and EB are 5, 2 μg/ml, respectively) in the absence or presence of divalent cation (200 mmol/l Mg or Mn, or 2 μmol/l Cu) was deposited onto a freshly cleaved mica surface. Approximately 1 min later, the residual solution on the mica was carefully removed by a slice of filter paper, followed by air drying. Samples were examined in a nanoscope III (Digital Instruments), and all images were recorded in a Tapping-mode operating at height-mode. The scan rate was usually set to 1.0–2.5 Hz.

3. Results and discussion

3.1. Direct observation of DNA condensation

Fig. 1 shows the typical AFM images of DNA, EB-DNA and EB-DNA-metal complex. The DNA molecule alone showed an extended line state, which is large, 0.8 nm in height and 12 nm in width, respectively (Fig. 1(A)), and corresponded to a typical double-stranded DNA tractate [12]. DNA–EB complex was still in an extended and isolated state, but there are also some coiled and tangled parts (Fig. 1(B)). The average height of these particles was 0.95 ± 0.2 nm and the average width was 15 nm, and greater than the diameter of duplex DNA. When EB was intercalated, the base pairs undergo an unwinding from an angle of 30° to one of 10° [13]. Although the overall base-stacking pattern was not disturbed, the strain produced during this process must be compensated. Therefore, parts along the strand were twisted together by supercoiling. But it was different to denatured DNA, which showed a random coiling (Fig. 1(C)).

When divalent cations are added, the single linear molecule disappears completely in the field of vision, and is replaced by various unusual structures. The addition of Cu (II) resulted in a complex network structure on the mica, and their average height was 1.0 ± 0.5 nm (Fig. 1(F)). The addition of Mg (II) ion resulted in composed of three or four maggot-like branch crossings at the same point. Close scrutiny reveals that there are some bead-like particles embedded in each branch (Fig. 1(D)). The average height of these particles was 17 ± 5 nm, which was significantly higher than those of double-stranded DNA under the same conditions. Under the existence of Mn (II) (Fig. 1(E)), most of them are in a semicircular shape, strong aggregation makes it difficult to measure the dimension of a separate one, but the average height of these particles was approximately 15 ± 6 nm.

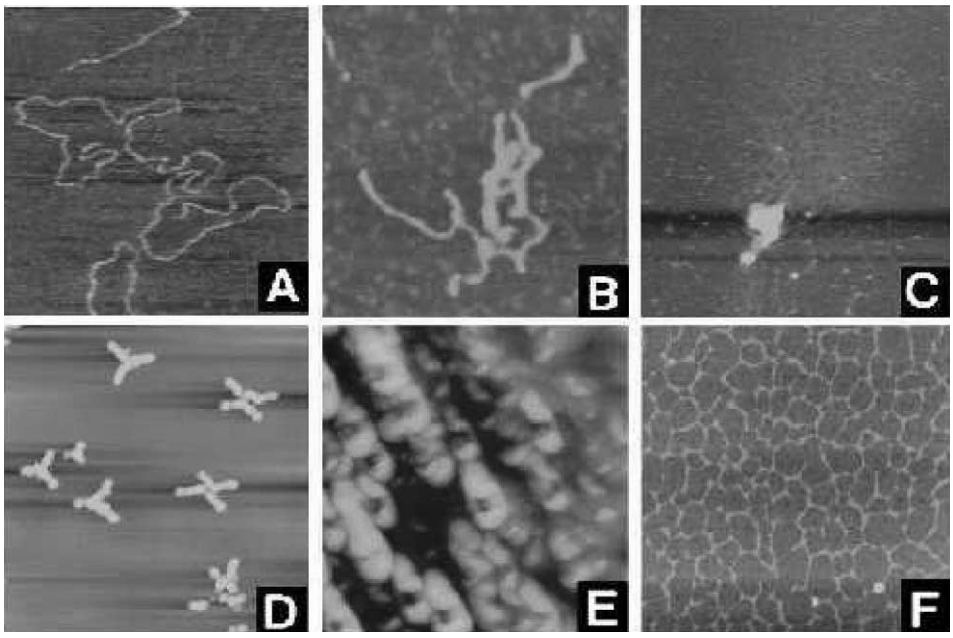

Fig. 1. AFM images of DNA. (A) DNA; (B) DNA + EB; (C) denatured DNA; (D) DNA + EB + Mg (II); (E) DNA + EB + Mn (II); (F) DNA + EB + Cu (II). The scan sizes of A, B, C, D, E and F image are 750×750 nm, 750×750 nm, 750×750 nm, 5×5 μm, 2.5×2.5 μm and 6×6 μm. Effects of metal ion-binding position on DNA condensation.

The above results from the AFM images indicated three divalent cations, Cu (II) Mg (II) and Mn (II) could induce the DNA condensation, but the morphologies induced are different in the morphologies in the presence of three divalent cations. Compared with previous work, a semicircular shape by Mn is somewhat similar to the condensated DNA structure (average height approximately 3 nm) induced by spermidine [14,15], $Co(NH_3)_6^{3+}$ [16] and organosilanes etc. [17,18]; three or four maggot-like branch crossing structures by Mg are somewhat similar to some V- and Y-shaped chromatin structures (average height 12 ± 2 nm) under high NaCl salt conditions [19], but the average height of these particles in this work was significantly higher. This implies that the structures observed in our experiment probably share the same forming mechanism, the difference in the shape maybe be related with the kind of cations and the detected system.

3.2. Effects of metal ion-binding position on DNA condensation

As shown in Fig. 2(A) and (B), EB–DNA fluorescence is progressively reduced by the addition of the three divalent metal ions, but the reduced degrees are various according to the ion type, and the fluorescence intensity decreased in this order Cu (II) > Mn (II) > Mg (II). Copper (II) has the biggest influence on the EB–DNA system. In the range of 0.0–0.5 μmol/l concentration, the fluorescence is quenched very sharply. Above 0.5 μmol/l, the change tends to be slow, and at 5 μmol/l it reaches a point where the residual fluorescence is almost identical to that of free EB. While for Mg (II) or Mn (II), no obvious fluorescence change is observed below 1 mmol/l and even at the highest concentration (400 mmol/l), the fluorescence is still three times higher than that of free EB. Results suggest that Cu is mainly bound to base pair, to influence the intercalation of EB molecular, and thus, led to the obvious decrease of fluorescence intensity. However, Mg (II) and Mn (II) are mainly bound to the phosphates of DNA, to infer the EB bound by electrostatic action, so no obvious fluorescence change is observed. As with the former results, the quantum yield also drops in the order Cu > Mn > Mg when divalent cations are added [Fig. 2(C)]. This indicates that the fluorescence change not only originates from the decreased number of the bound ligands, but also relates to the energy transfer efficiency. In other words, after metal ions are bound, the relative orientation between EB and DNA is affected. Hence, the plane of the intercalated molecule cannot be parallel to the DNA base pairs well, and the energy transfer is not so effective as that in the absence of these ions. Moreover, the more stronger the metal ions interact with the base, the lower the energy transfer is.

Fig. 2 showed the CD spectra of DNA and its complexes with EB under different conditions. Here it can be seen that native calf thymus DNA gives a typical CD spectrum of B-type DNA with the positive band at 278 nm and the negative band at 252 nm [20]. After the binding of EB, this spectrum is altered significantly. A new complex band with a maximum near 308 nm and a

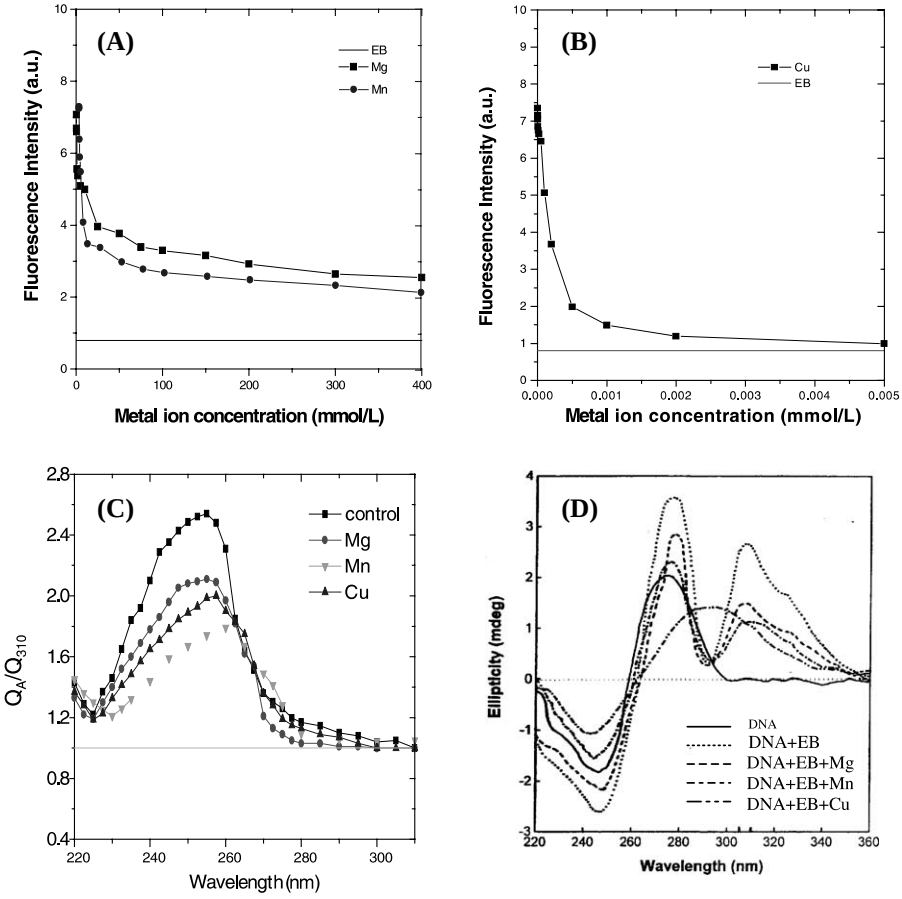

Fig. 2. (A) and (B) Fluorescence change of the EB–DNA complex in the presence of Mg (II), Mn (II) and Cu. (C) The relative fluorescence quantum yield of DNA–EB complex in the presence and absence of divalent metal cation. The concentrations of Mg (II), Mn (II) and Cu (II) are chosen at 50, 5 and 0.25 μmol/l, respectively. In this case, the fluorescence of EB–DNA is half reduced. The concentrations of DNA and EB are 5 and 2 μg/ml, respectively. (D) Circular dichroism spectra of DNA and EB–DNA. The concentration of DNA is 50 and 20 μg/ml, respectively. The concentrations of Mg, Mn (II) and Cu (II) are 200, 200 and 2 μmol/l, respectively.

shoulder at 325 nm appears. From previous studies, we know that the spectrum in this range is independent of nucleic acid, its shape tends to be conservative whatever the sequence is, and ellipticities are directly related to the ratio of added ethidium to polynucleotide phosphate. Therefore, to some extent it could be exploited as a "signature" for the intercalation of EB to DNA. According to Johnson et al. [21], the behavior of the CD bands at ≈280 nm is the most reliable means of following conformational variation in DNA. Similar spectra were also shown by the EB–DNA systems containing Mg (II) or Mn (II) ion. The only difference lies in the amplitude. Ellipticities, examined along the wavelength, were decreased in the presence of these divalent cations. Since ion binding can enhance the base stacking, the local environment was altered, resulting in the transition of conformation. Nevertheless, the overall structure of the complex still maintains B type conformation. In the case of Cu (II) ion, a broad positive band with a maximum of nearly 289 nm was manifested between 260 and 360 nm instead of the characteristic peak at 308 nm accompanying the intercalation. Such a shape is somewhat similar to that of the interaction between EB and a single-strand nucleotide. It is known that a Cu (II) ion can induce DNA molecules to partially denature. Thus it is conceivable that some parts of the double-stranded helix exist in a separate state. This is consistent with the much decreased negative band at 246 nm, which served as the feature of DNA denaturation, and also adds credence to this presumption. The distinct CD spectrum observed further showed that the binding point between DNA and three cations is different. It is also indicated that a higher ordered self-organization was involved in their formation.

3.3. Stability of DNA condensation

Besides the static spectrum, thermal denaturation provides additional evidence for different influences of these ions on DNA condensation. As shown in Fig. 3, DNA alone exhibits a broad helix–coil transition. Upon binding with EB, it is effectively stabilized and shows a

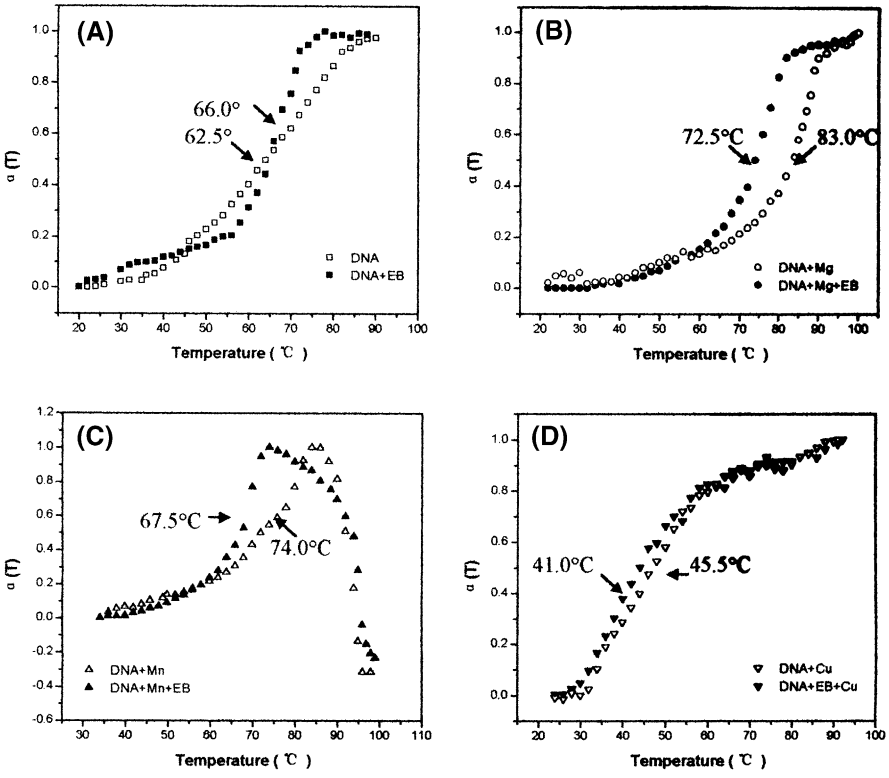

Fig. 3. Thermal denaturation profiles for DNA under different condtions. The concentrations of DNA and EB are 5 and 2 μg/ml, respectively. The concentrations of Mg (II), Mn (II) and Cu (II) are 200, 200 and 2 μmol/l, respectively.

sharp transition, because the intercalated EB is aligned in a manner permitting the formation of hydrogen bonds between the amino groups of the ring and charged oxygen of the phosphate groups of both strands. Thus, in order to separate them, more energy is required, which consequently increased the T_m (Fig. 3(A)). When Mg (II) was added into this binary system, the situation becomes complex in that simultaneous incubation of DNA (Fig. 3(B)), Mg (II) and EB can result in a kinetic competition between binding of DNA with Mg (II) and with EB. Moreover, both of them can stabilize DNA [22]. Thus, the coexisted two bindings cooperatively increase the T_m. By comparison, we found the latter most likely occurs since the T_m of this system is higher than that of DNA–EB, but lower than that of DNA–Mg (II), indicating a compromised result of the two bindings. Like Mg (II), Mn (II) exerts a similar influence on the T_m of DNA–EB, with the most pronounced difference being the shape of the melting profile, shown in Fig. 3(C). The absorbency dropped dramatically after reaching the maximum. This is presumably due to DNA aggregation since turbidity is observed during melting. As the temperature increases, the aggregated particles induced by Mn (II) will become larger and larger, eventually subside, and result in a decrease of absorbency. In contrast to Mg and Mn, the T_m of DNA–Cu remains unchanged in the presence or absence of EB. Moreover, both of the T_m are much lower than that of DNA alone. The lack of any EB effect on the thermal denaturation and the relatively low T_m value prove that DNA is partially denatured [23]. This is why Cu effect is obviously different to the other cation. Therefore, no stabilization to DNA is observed.

Above results show that Cu^{2+}, Mn^{2+} and Mg^{2+} ions with the same valence have the different morphologies in inducing DNA condensation. The main reason is probably due to the binding site of the metal ion. From previous experiments, it was found that the divalent cations bind preferentially to the bases relative to phosphates in the following order, $Cu^{2+} > Pd^{2+} > Cd^{2+} > Zn^{2+} > Mn^{2+} > Co^{2+}$, $Ni^{2+} > Fe^{2+} > Ca^{2+} > Mg^{2+}$, Ba^{2+}. AFM images obtained can be explained. Since Cu (II) can coordinate with the electron-rich sites on the base, its binding can strongly disrupt the base pair, thus greatly interfering with the intercalation of EB. Its binding at the primary sites is proposed to locally destabilize the double helix. The metal-bound bases may then serve as an additional nucleation site to link with other available base acceptors. This mechanism would allow separated DNA strands or their separated local domains, to crosslink. Extension of the crosslinking would eventually lead to a network as shown in Fig. 1(F) [24].

Mg (II), the typical divalent cation binding to phosphate, can neutralize the negative charge of sugar–phosphate backbone, lead to the reduction of the

electrostatic attraction of DNA to EB and decrease of the fluorescence. As noted above, the binding of EB can unwind the DNA helix by about 20°, thus lengthening the molecule and making it prone to self-coiling. After Mg (II) ion is added, this tendency was further enhanced. Once a condensed nucleus is formed, the hydration force will drive the remaining part to wind around it, then form a bead-like particle. As this nucleation and growth process continues, a sting of the particles will appear (Fig. 1(D)). It is not clear, as yet, why they cross at a point.

The Mn (II) has been reported to interact with both phosphate and base. In our experiment its effect was between Cu (II) and Mn. However, its behavior is much similar to Mg (II), not Cu (II), although both of them are transition metals. This may be related to its electronic distribution. Studies found that some toroids are actually formed by bending rods since these rods are in essence not stiff but rather flexible entities, which can coil up into annular structures if end to end aggregation is strong enough for stabilization [25]. For Mn, the energy required for the abrupt bending is not enough to complete the transition, thus it terminates in an unclosed circle, to form the semicircular shape. This implies that the structures observed in our experiment probably share the same forming mechanism as to the role of EB in this process, it remains to be determined.

In contrast such a condensate has never been observed in the DNA solution containing only the metal ion or EB. Thus, we presume that it probably results from the cooperative effect of the two ligands. Although the cation concentrations used in our experiments are considerably higher than that in vivo, it is conceivable that compartmentalization, synergistic interactions or presentation by accessory molecules could facilitate their interaction with nucleic acids under appropriate conditions. Alternatively, the effects of the divalent cations in vitro might well be duplicated naturally within the cell by polyamines or a specialized basic polypeptide domain [26–28]. Therefore, the data presented here provide a possibility that by modulating the cation type and its concentration in a local environment, we can gain an optimal curative effect of the drug whose target is nucleic acid.

Acknowledgements

We are indebted to the financial support from the foundation of Academia Sinica, and support from a grant from National Science Foundation of China (30170246).

References

[1] H. Sigel, in: T.D. Tullius (Ed.), Metal-DNA Chemistry, American Chemical Society, Washington, DC, 1989, pp. 159–204.
[2] J.G. Duguid, V.A. Bloomfield, J.M. Benevides, G.J. Thomas, Biophys. J. 69 (1995) 2623.
[3] C. Ma, V.A. Bloomfield, Biophys. J. 67 (1994) 1678.
[4] J.G. Duguid, V.A. Bloomfield, Biophys. J. 69 (1995) 2642.
[5] V.V. Andrushchenko, S.V. Kornilova, L.E. Kapinos, E.V. Hackl, V.L. Galkin, D.N. Grigoriev, J. Mol. Struct. 408–409 (1) (1997) 225–228.
[6] E.V. Hackl, S.V. Kornilova, L.E. Kapinos, V.V. Andrushchenko, V.L. Galkin, D.N. Grigoriev, J. Mol. Struct. 408–409 (2) (1997) 229–232.
[7] H. Arkawa, R. Ahamad, M. Naoui, H.A. Tajmir-Rjahi, J. Biol. Chem. 275 (2000) 1050–1053.
[8] Chunli Bai, Chen Wang, Zhang, Lin, Sci. Found. China 7 (1999) 47–50.
[9] L.D. Williams, I.H. Goldberg, Biochemistry 27 (1988) 3004.
[10] B.H. Geierstranger, M. Mrksich, P.B. Dervan, D.E. Wemmer, Science 266 (1994) 646.
[11] K.M. Hyunm, S.D. Choi, S. Lee, S.K. Kim, Biochem. Biophys. Acta 1334 (1997) 312.
[12] H. Hansma, G.I. Revenko, K. Kim, D.E. Laney, Nucleic Acids Res. 24 (1996) 713.
[13] J.E. Coury, L.M. Ison, L.D. Williams, L.A. Bottomley, Proc. Natl. Acad. Sci. USA 93 (1996) 12283.
[14] Z. Lin, C. Wang, X. Feng, M. Liu, J. Li, C. Bai, Nucleic Acids Res. 26 (1998) 3228.
[15] Y. Fang, J.H. Hoh, J. Am. Chem. Soc. 120 (1998) 8903.
[16] D. Liu, C. Wang, Z. Lin, J. Li, B. Xu, Z. Wei, Z. Wang, C. Bai, Surf. Interface Anal. 32 (1) (2001) 15–19.
[17] Y. Fang, J.H. Hoh, Nucleic Acids Res. 26 (1998) 588.
[18] A.L. Martin, M.C. Davies, B.J. Rackstraw, C.J. Roberts, S. Stolnik, S.J.B. Tendler, P.M. Williams, FEBS Lett. 480 (2–3) (2000) 106–112.
[19] D. Liu, C. Wang, J. Li, Z. Wang, B. Xu, Z. Wei, Z. Lin, J. Qin, E.H. Cao, C. Bai, Surf. Interface Anal. 32 (1) (2001) 20–26.
[20] X.G. Sun, E.H. Cao, Y.J. He, J.F. Qin, J. Biomol. Struct. Dyn. 16 (1999) 863.
[21] B.B. Johnson, K.S. Dahl, J.I. Tinocco, V.I. Ivanov, V.B. Zhurkin, Biochemistry 20 (1981) 73.
[22] Q. Guo, M. Lu, L.A. Marky, N.R. Kallenbach, Biochemistry 31 (1992) 2451.
[23] W. Forster, E. Bauer, H. Schutz, Biopolymer 18 (1979) 625.
[24] J.G. Duguid, V.A. Bloomfield, Berg, J.M. Benevides, G.J. Thomas, Biophys. J. 65 (1993) 1916.
[25] P.G. Arscott, V.A. Bloomfield, in: O.M. Marti, M. Amrein (Eds.), STM and SFM in Biology, Academic Press, California, 1993, pp. 259–270.
[26] Blume Lebowitz, S.W.V. Guarcello, W. Zacharias, D.M. Miller, Nucleic Acids Res. 25 (1997) 617.
[27] S.W. Zacharias, J.D.M. Guarcello, W.V. Miller, Nucleic Acids Res. 27 (1999) 695.
[28] R.L. Hettich, Int. J. Mass Spectrom. 204 (1–3) (2001) 55–75.